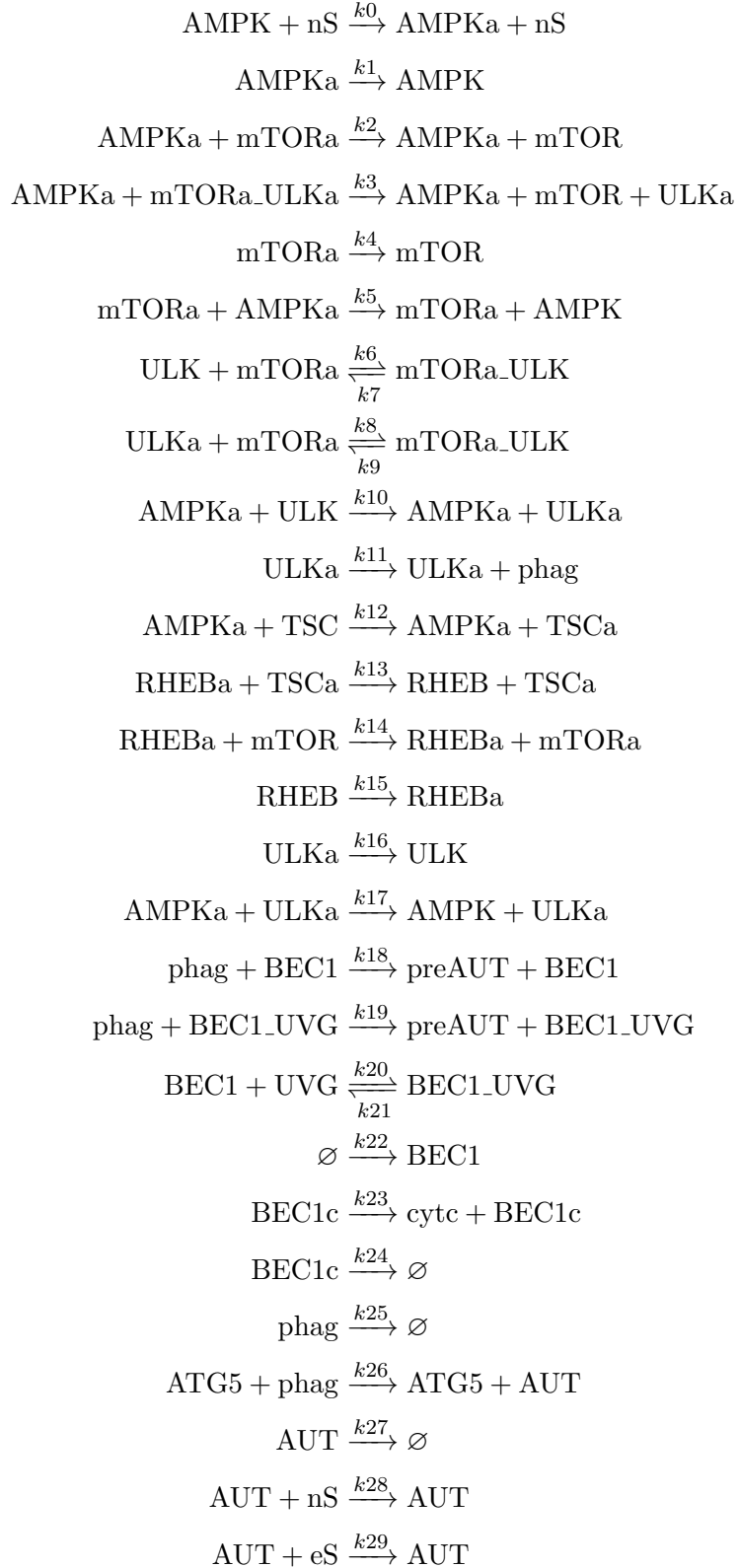
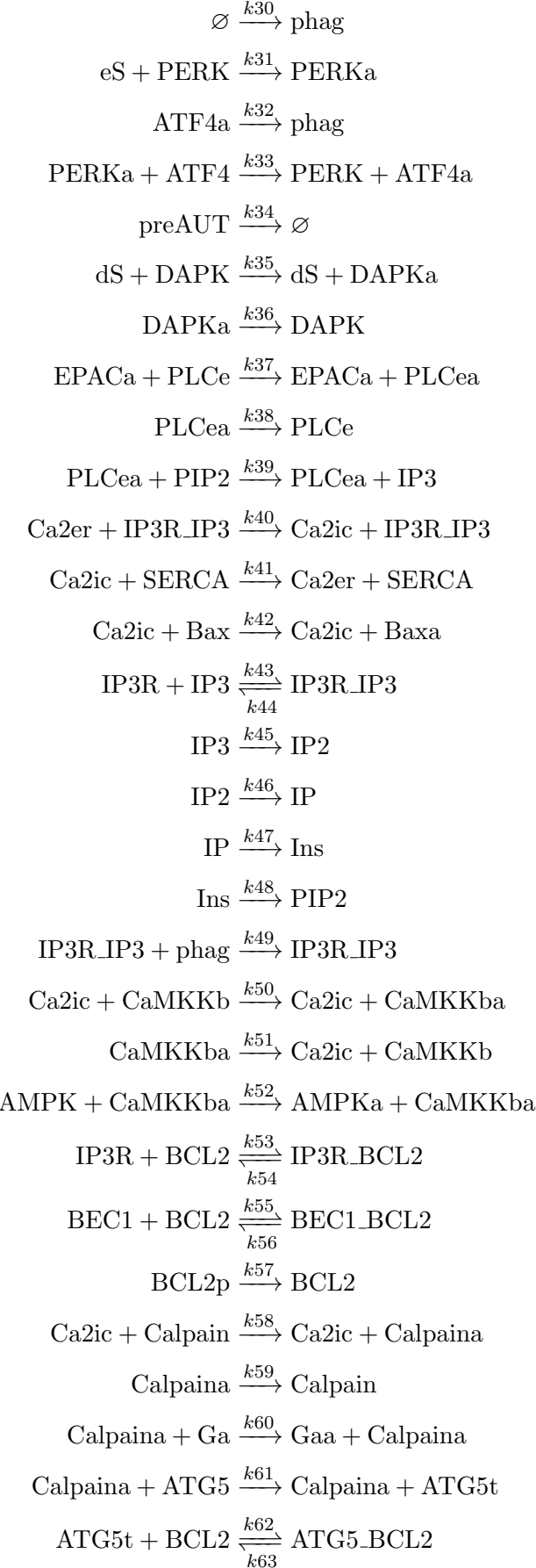
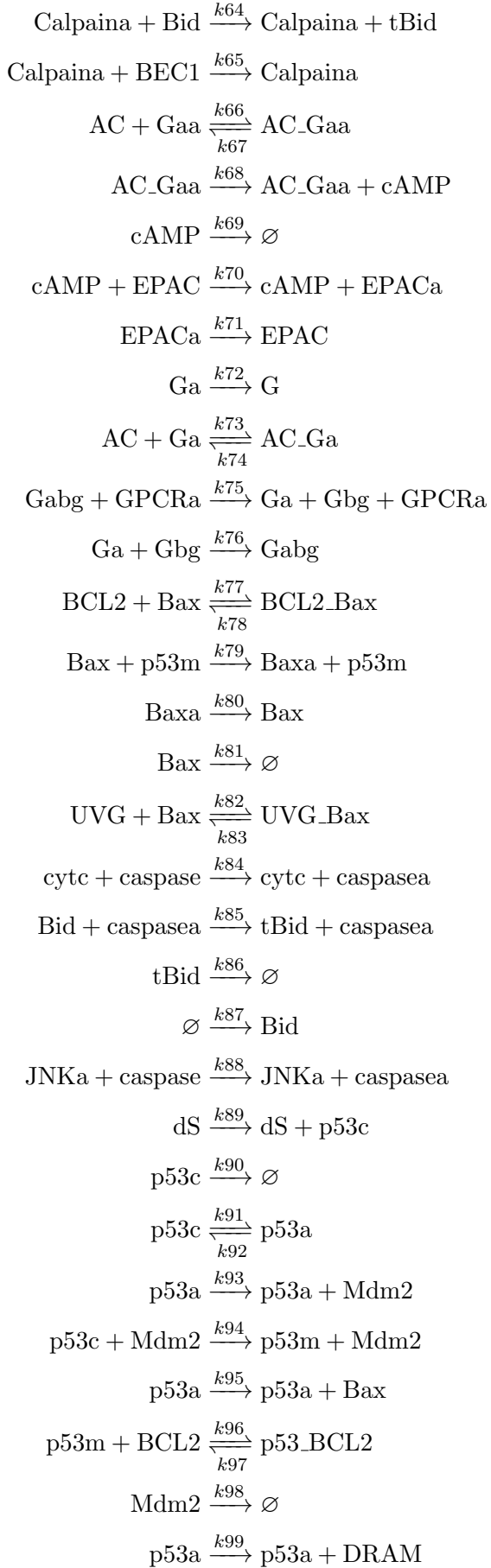


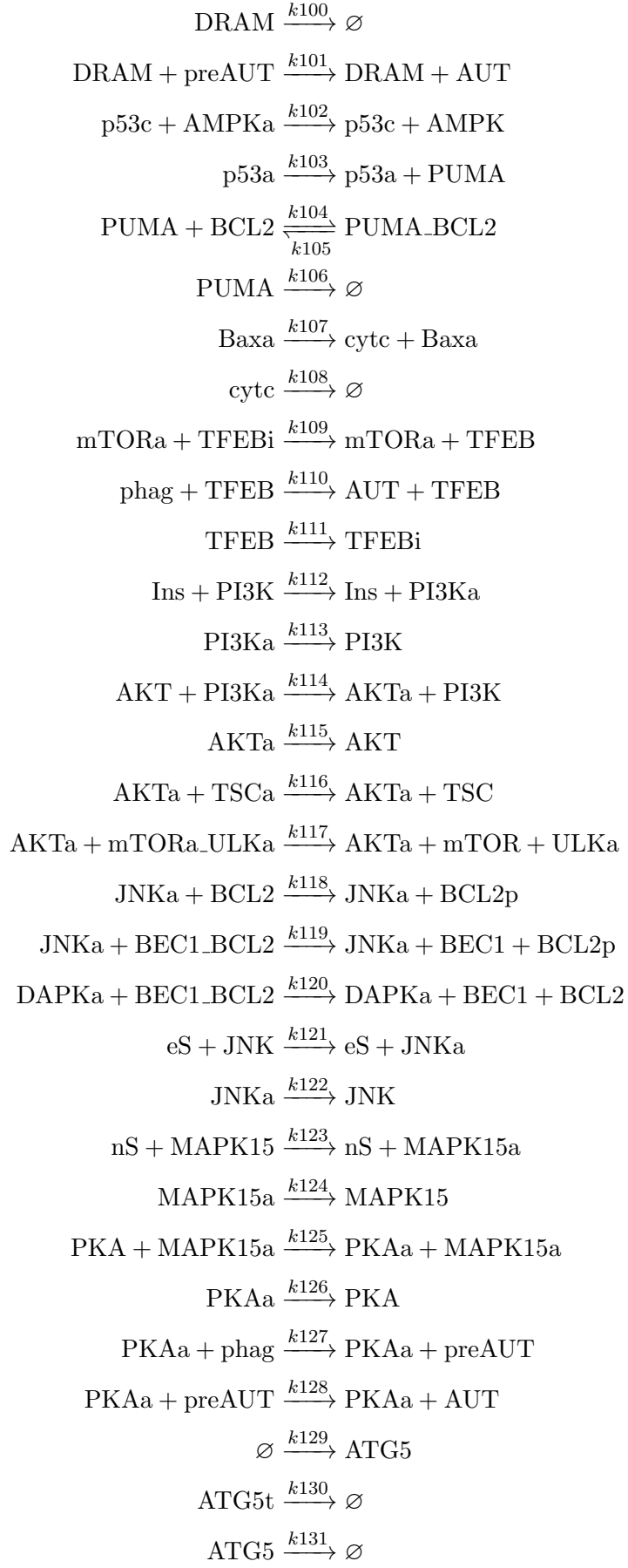
1 Liu et al. model's original reactions

The calculations were carried out in $\frac{mol}{cm^3}$, thus the rate coefficients values for the first and second order reactions are taken in $\frac{1}{s}$ and $\frac{cm^3}{mol*s}$ units, respectively.



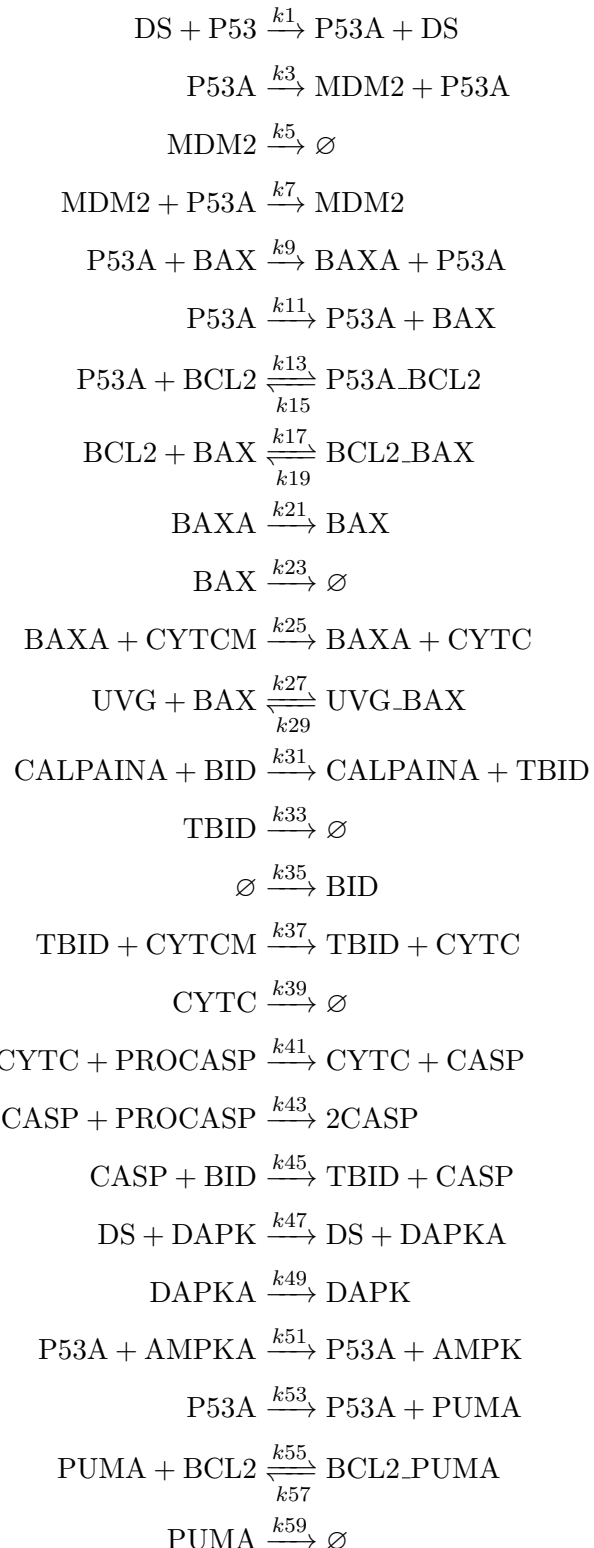


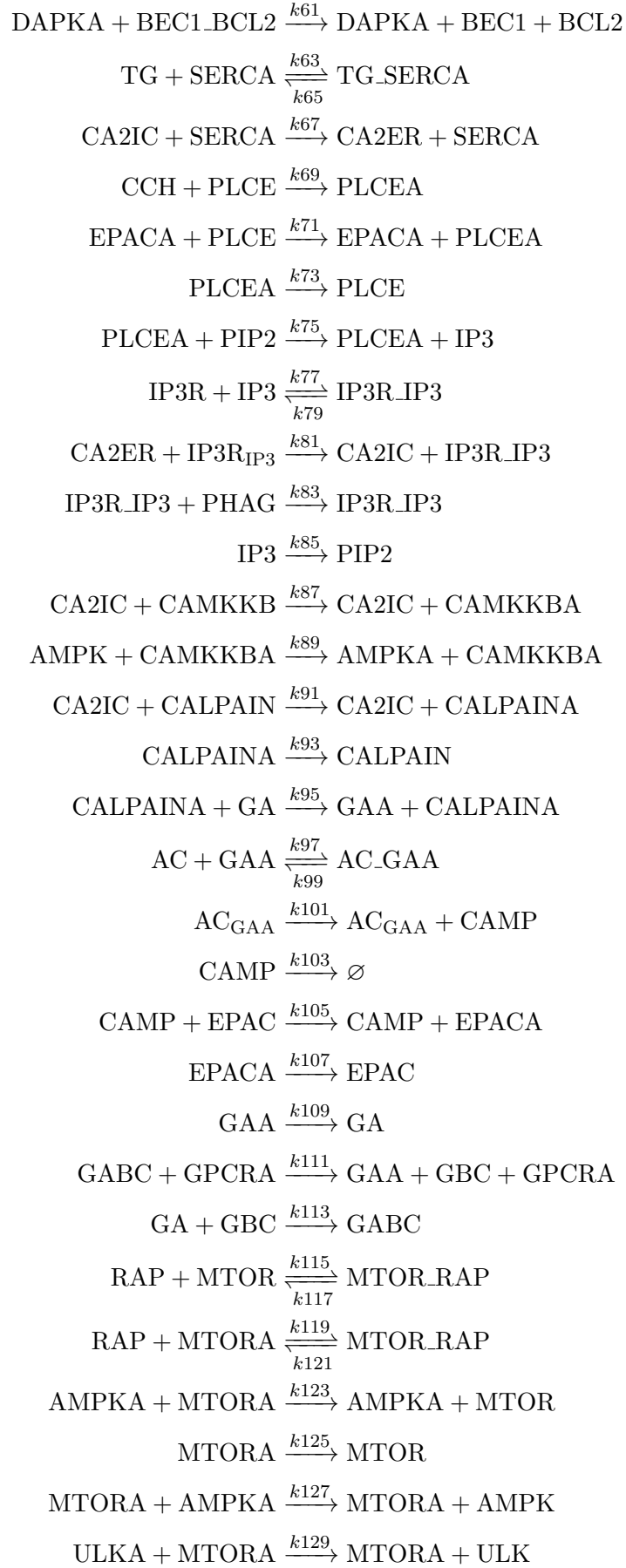


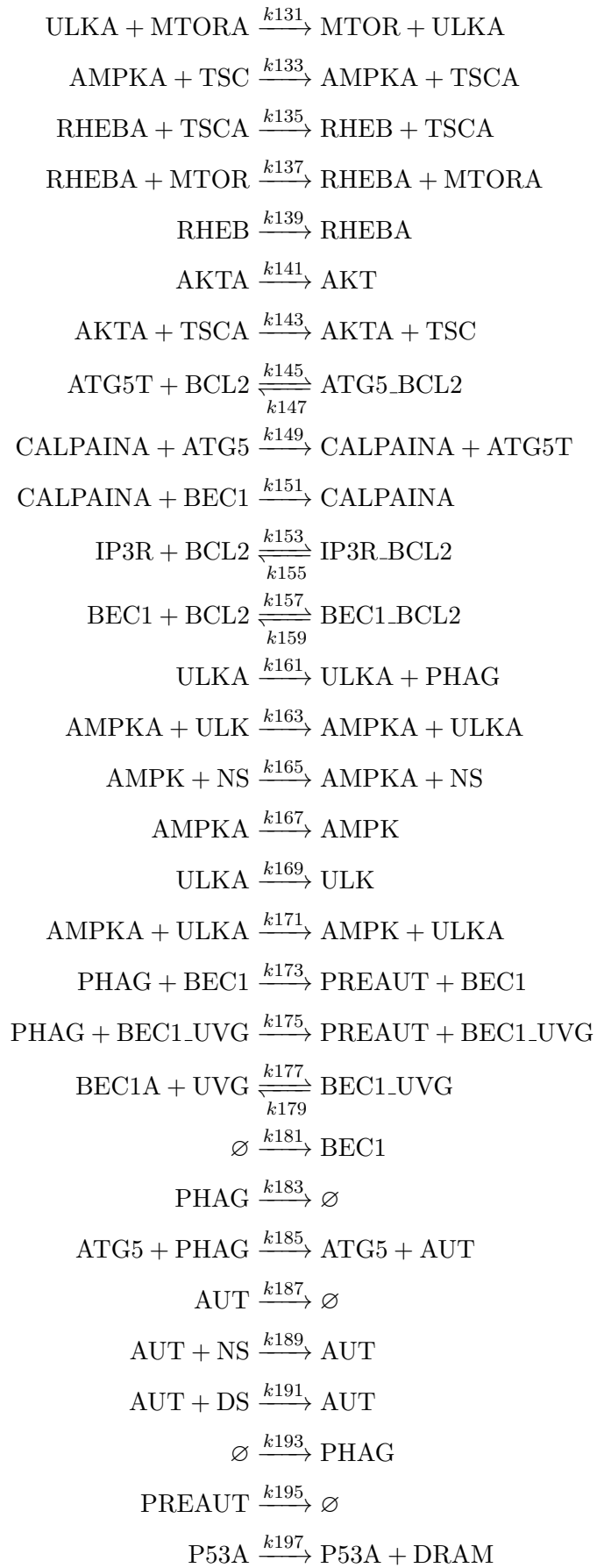


2 Revised reactions

The calculations were carried out in $\frac{mol}{cm^3}$, thus the rate coefficients values for the first and second order reactions are taken in $\frac{1}{s}$ and $\frac{cm^3}{mol*s}$ units, respectively.







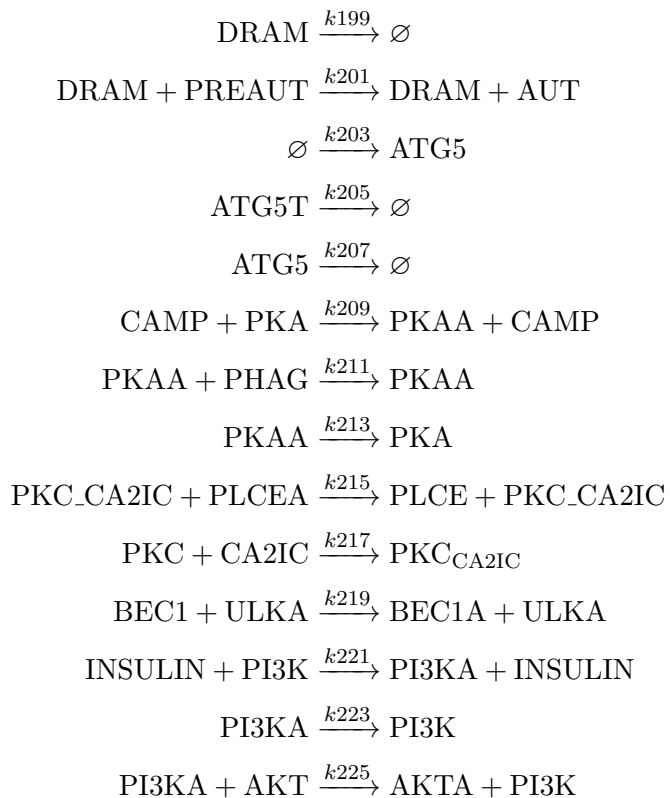


Table S1: List of the species found in the models, and their full names

Short Notation	Full Name
AMPK	AMP-activated protein kinase
nS	Nuclear Stress
AMPKa	Active AMP-activated protein kinase
mTORa	Active mammalian target of rapamycin
mTOR	mammalian target of rapamycin
mTOR_ULK	mTOR ULK complex
ULKa	Active Unc-51 like autophagy activating kinase
ULK	Unc-51 like autophagy activating kinase
phag	Phagophore
TSC	Tuberous sclerosis complex
TSCa	Active tuberous sclerosis complex
RHEBa	Active Ras homolog enriched in brain
RHEB	Ras homolog enriched in brain
BEC1	Beclin 1
preAUT	Pre-autophagosome
BEC1_UVG	Beclin 1 UVRAG complex
UVG	UV radiation resistance-associated gene
BEC1c	Cytosolic Beclin 1
cytc	Cytochrome c

Table S1: List of the species found in the models, and their full names

Short Notation	Full Name
ATG5	Autophagy-related protein 5
AUT	Autophagosome
eS	ER Stress
PERK	Protein kinase R-like endoplasmic reticulum kinase
PERKa	Active PERK
ATF4a	Active Activating Transcription Factor 4
ATF4	Activating Transcription Factor 4
dS	DNA Stress
DAPK	Death-associated protein kinase
DAPKa	Active death-associated protein kinase
EPACa	Active exchange protein directly activated by cAMP
PLCe	Phospholipase C epsilon
PLCea	Active phospholipase C epsilon
PIP2	Phosphatidylinositol 4,5-bisphosphate
IP3	Inositol trisphosphate
Ca2er	Endoplasmic reticulum calcium ion
IP3R_IP3	IP3 receptor IP3 complex
Ca2ic	Intracellular calcium
SERCA	Sarcoplasmic/endoplasmic reticulum calcium ATPase
Bax	Bcl-2-associated X protein
Baxa	Active Bcl-2-associated X protein
IP3R	IP3 receptor
IP2	Inositol bisphosphate
IP	Inositol phosphate
Ins	Insulin
CaMKKb	Calcium/calmodulin-dependent protein kinase kinase beta
CaMKKba	Active calcium/calmodulin-dependent protein kinase kinase b
BCL2	B-cell lymphoma 2
IP3R_BCL2	IP3 receptor BCL2 complex
BEC1_BCL2	Beclin 1 BCL2 complex
BCL2p	Phosphorylated BCL2
Calpain	Calpain
Calpaina	Active calpain
Ga	G protein alpha subunit
Gaa	Active G protein alpha subunit
ATG5t	truncated ATG5
ATG5_BCL2	ATG5 BCL2 complex
Bid	BH3 interacting-domain death agonist
tBid	Truncated Bid

Table S1: List of the species found in the models, and their full names

Short Notation	Full Name
AC	Adenylate cyclase
AC_Gaa	Adenylate cyclase G protein alpha subunit complex
cAMP	Cyclic adenosine monophosphate
EPAC	Exchange protein directly activated by cAMP
G	G protein
AC_Ga	Adenylate cyclase G protein alpha subunit complex
Gabg	G protein alpha, beta, gamma subunits
GPCRa	Active G protein-coupled receptor
Gbg	G protein beta and gamma subunits
BCL2_Bax	BCL2 Bax complex
p53m	Mitochondrial p53
UVG_Bax	UVG bound to Bax
caspase	Procaspsase
caspasea	Cleaved caspase
JNKA	Active c-Jun N-terminal kinase
p53c	Cytosolic p53
p53a	Active p53
Mdm2	Mouse double minute 2 homolog
p53_BCL2	p53 BCL2 complex
DRAM	DNA damage-regulated autophagy modulator
PUMA	p53 upregulated modulator of apoptosis
PUMA_BCL2	PUMA BCL2 complex
TFEBi	Inactive transcription factor EB
TFEB	Transcription factor EB
PI3K	Phosphoinositide 3-kinase
PI3Ka	Active phosphoinositide 3-kinase
AKT	Protein kinase B
AKTa	Active protein kinase B
JNK	c-Jun N-terminal kinase
MAPK15	Mitogen-activated protein kinase 15
MAPK15a	Active mitogen-activated protein kinase 15
PKA	Protein kinase A
PKAAa	Active protein kinase A

3 Initial protein concentrations

Table S2: Initial species concentration ranges in nM

species	min	max	source
AC	100	400	[1, 2]
AC_Ga	0	100	assumed
AC_Gaa	0	100	assumed
AKT	0	100	[3, 4]
AKTa	50	200	[3, 4]
AMPK	187.5	750	[5, 6]
AMPKa	0	100	[5, 6]
ATG5	100	400	[7]
ATG5_BCL2	0	100	assumed
ATG5t	15	60	assumed
AUT	0	100	[8]
BCL2	25	100	[9, 10]
BCL2_Bax	10	40	[9]
BCL2_PUMA	25	100	[9]
BEC1	50	200	[11]
BEC1_BCL2	0	100	assumed
BEC1_UVG	0	100	assumed
Bax	10	40	[9, 10]
Baxa	0	0	[9, 10]
Bid	10	40	[9, 10]
Ca2er	500	2000	[12, 13, 14]
Ca2ic	50	200	[12, 13, 14]
CaMKKb	50	200	[12]
CaMKKba	0	100	[12]
Calpain	10	40	[15]
Calpaina	0	100	[15]
DAPK	50	200	[11]
DAPKa	0	100	[11]
DRAM	0	100	[11]
EPAC	5	20	assumed
EPACa	0	100	assumed
GPCRa	5	20	[16]
Ga	5	20	[16, 17, 13]
Gaa	0	100	[16, 17, 13]
Gabc	0	100	[16, 17, 13]
Gbc	5	20	[16, 17, 13]
IP3	65	260	[12]
IP3R	5	20	[12]
IP3R_BCL2	0	100	assumed

IP3R_IP3	0	100	assumed
MDM2	0	100	[18, 19]
P53a_BCL2	0	100	assumed
PLCea	0	100	[12]
PLCe	5	20	[12, 14, 20]
PIP2	250	1000	[12]
PKA	75	300	[2]
PKAa	0	100	assumed
PUMA	0	100	assumed
RHEB	0	100	assumed
RHEBa	150	600	assumed
SERCA	0	100	[12]
TSC	112.5	450	[5, 6]
TSCa	0	100	[5, 6]
ULK	35	140	[8]
ULKa	0	100	assumed
UVG	50	200	assumed
UVG_Bax	0	100	assumed
cAMP	0	100	[1, 2]
casp	0	0	assumed
cytc	0	100	[9, 10]
cytcm	10	40	[9, 10]
mTOR	0	100	[5, 11]
mTORa	187.5	750	[5, 11]
mTORa_ULK	0	100	assumed
mTORa_ULKa	0	100	assumed
p53	12.5	50	[18, 19]
p53a	0	100	assumed
phag	0	100	assumed
preAUT	0	100	assumed
procasp	12	48	[9, 21]
tBid	0	100	[9]

References

- [1] Iancu, R.V.; Jones, S.W.; Harvey, R.D. Compartmentation of camp signaling in cardiac myocytes: A computational study. *Biophys. J.* **2007**, *92*, 3317–3331.
- [2] Nakano, T.; Doi, T.; Yoshimoto, J.; Doya, K. A kinetic model of dopamine- and calcium-dependent striatal synaptic plasticity. *PLoS Comput. Biol.* **2010**, *6*, e1000670.

- [3] Shin, S.-Y.; Nguyen, L. Unveiling hidden dynamics of hippo signalling: A systems analysis. *Genes* **2016**, *7*, 44.
- [4] Hat, B.; Kochańczyk, M.; Bogdał, M.N.; Lipniacki, T. Feedbacks, bifurcations, and cell fate decision-making in the p53 system. *PLOS Comput. Biol.* **2016**, *12*, e1004787.
- [5] Pezze, P.D.; Sonntag, A.G.; Thien, A.; Prentzell, M.T.; Gödel, M.; Fischer, S.; Neumann-Haefelin, E.; Huber, T.B.; Baumeister, R.; Shanley, D.P.; et al. A dynamic network model of mtor signaling reveals tsc-independent mtorc2 regulation. *Sci. Signal.* **2012**, *5*, ra25.
- [6] Varusai, T.M.; Nguyen, L.K. Dynamic modelling of the mtor signalling network reveals complex emergent behaviours conferred by deptor. *Sci. Rep.* **2018**, *8*, 643.
- [7] Broadbent, D.G.; Barnaba, C.; Perez, G.I.; Schmidt, J.C. Quantitative analysis of autophagy reveals the role of atg9 and atg2 in autophagosome formation. *J. Cell Biol.* **2023**, *222*, e202210078.
- [8] du Toit, A.; Hofmeyr, J.-H.S.; Gniadek, T.J.; Loos, B. Measuring autophagosome flux. *Autophagy* **2018**, *14*, 1060–1071.
- [9] Bagci, E.Z.; Vodovotz, Y.; Billiar, T.R.; Ermentrout, G.B.; Bahar, I. Bistability in apoptosis: Roles of bax, bcl-2, and mitochondrial permeability transition pores. *Biophys. J.* **2006**, *90*, 1546–1559.
- [10] Raychaudhuri, S.; Das, S. Low probability activation of bax/bak can induce selective killing of cancer cells by generating heterogeneity in apoptosis. *J. Healthc. Eng.* **2013**, *4*, 47–66.
- [11] Tavassoly, I.; Parmar, J.; Shajahan-Haq, A.N.; Clarke, R.; Baumann, W.T.; Tyson, J.J. Dynamic modeling of the interaction between autophagy and apoptosis in mammalian cells. *CPT Pharmacometr. Syst. Pharmacol.* **2015**, *4*, 263–272.
- [12] Dolan, A.T.; Diamond, S.L. Systems modeling of ca₂₊ homeostasis and mobilization in platelets mediated by ip3 and store-operated ca₂₊ entry. *Biophys. J.* **2014**, *106*, 2049–2060.
- [13] Lemon, G.; Gibson, W.G.; Bennett, M.R. Metabotropic receptor activation, desensitization and sequestration—i: Modelling calcium and inositol 1,4,5-trisphosphate dynamics following receptor activation. *J. Theor. Biol.* **2003**, *223*, 93–111.
- [14] Wang, J.; Huang, X.; Huang, W. A quantitative kinetic model for atp-induced intracellular oscillations. *J. Theor. Biol.* **2007**, *245*, 510–519.
- [15] Ashraf, J.; Ahmad, J.; Ul-Haq, Z. *Deciphering the Role of PKC in Calpain-CAST System Through Formal Modeling Approach*; Springer International Publishing: Berlin/Heidelberg, Germany, 2019; pp. 60–71.

- [16] Smith, B.; Hill, C.; Godfrey, E.L.; Rand, D.; van den Berg, H.; Thornton, S.; Hodgkin, M.; Davey, J.; Ladds, G. Dual positive and negative regulation of gpcr signaling by gtp hydrolysis. *Cell. Signal.* **2009**, *21*, 1151–1160.
- [17] Tiveci, S.; Akin, A.; Çakır, T.; Saybaşılı, H.; Ülgen, K. Modelling of calcium dynamics in brain energy metabolism and alzheimer’s disease. *Comput. Biol. Chem.* **2005**, *29*, 151–162.
- [18] Chong, K.H.; Samarasinghe, S.; Kulasiri, D. Mathematical modelling of p53 basal dynamics and dna damage response. *Math. Biosci.* **2015**, *259*, 27–42.
- [19] Geva-Zatorsky, N.; Rosenfeld, N.; Itzkovitz, S.; Milo, R.; Sigal, A.; Dekel, E.; Yarnitzky, T.; Liron, Y.; Polak, P.; Lahav, G.; et al. Oscillations and variability in the p53 system. *Mol. Syst. Biol.* **2006**, *2*, 2006.0033.
- [20] Eungdamrong, N.J.; Iyengar, R. Compartment-specific feedback loop and regulated trafficking can result in sustained activation of ras at the golgi. *Biophys. J.* **2007**, *92*, 808–815.
- [21] Neumann, L.; Pforr, C.; Beaudouin, J.; Pappa, A.; Fricker, N.; Krammer, P.H.; Lavrik, I.N.; Eils, R. Dynamics within the cd95 death-inducing signaling complex decide life and death of cells. *Mol. Syst. Biol.* **2010**, *6*, 352.